



An Efficient Optimization of a Burst Mode-operated Fabry Perot Cavity for Compton Light sources

Vlad Musat, Andrea Latina, Eduardo Granados (CERN), Eric Cormier, Giorgio Santarelli (LP2N)

29/08/2023

Contents

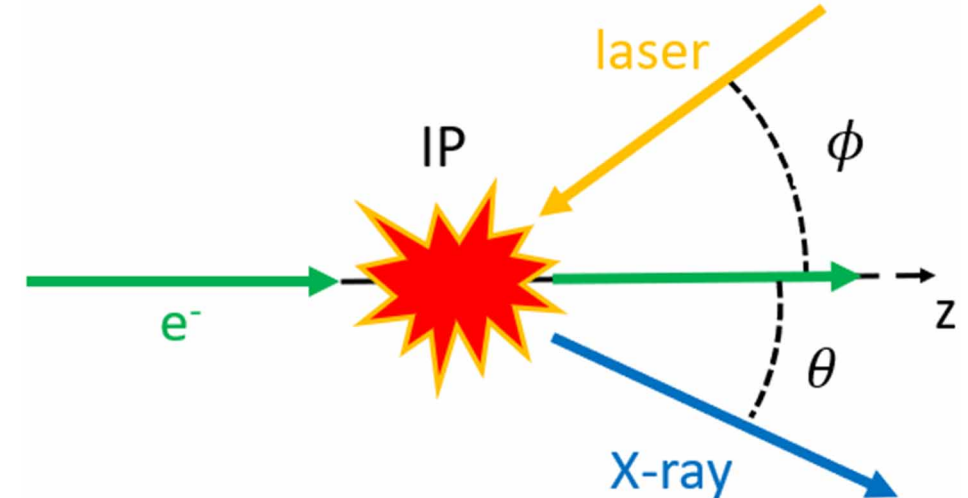
- 1. Theoretical background**
- 2. Burst mode parameters of the Fabry-Perot cavity**
- 3. Geometry of the Fabry-Perot cavity**
- 4. Impact of thermal effects**
- 5. Example case: HPCI Compton Light source**



Inverse Compton Scattering

= The scattering of a **low energy photon** from an EM field to a **high-energy photon** (X-ray or gamma ray) during the interaction with a **charged particle**.

One of the few compact light sources capable of generating MeV photons with a small energy bandwidth.



$$N_\gamma = \sigma_c \frac{N_e N_{\text{laser}} \cos(\phi/2)}{2\pi \sigma_{\gamma,y} \sqrt{\sigma_{\gamma,x}^2 \cos^2(\phi/2) + \sigma_{\gamma,z}^2 \sin^2(\phi/2)}}$$

Total flux

$$\frac{\sigma_{E_\gamma}}{E_\gamma} = \sqrt{\left(\frac{\sigma_{E_\theta}}{E_\theta}\right)^2 + \left(2\frac{\sigma_{E_e}}{E_e}\right)^2 + \left(\frac{\sigma_{E_{\text{laser}}}}{E_{\text{laser}}}\right)^2 + \left(\frac{\sigma_{E_\epsilon}}{E_\epsilon}\right)^2}$$

Photon bandwidth

$$\mathcal{B} = \frac{\mathcal{F}}{4\pi^2 \sigma_{\gamma,x} \sqrt{\epsilon_x/\beta_x} \sigma_{\gamma,y} \sqrt{\epsilon_y/\beta_y}}$$

Average brilliance

$$E_{\text{X-ray}} = 2\gamma^2 E_{\text{laser}} \frac{1 + \cos \phi}{1 + \gamma^2 \theta^2}$$

Photon energy

How to maximise the photon flux?

$$N_\gamma = \sigma_c \frac{N_e N_{\text{laser}} \cos(\phi/2)}{2\pi \sigma_{\gamma,y} \sqrt{\sigma_{\gamma,x}^2 \cos^2(\phi/2) + \sigma_{\gamma,z}^2 \sin^2(\phi/2)}}$$

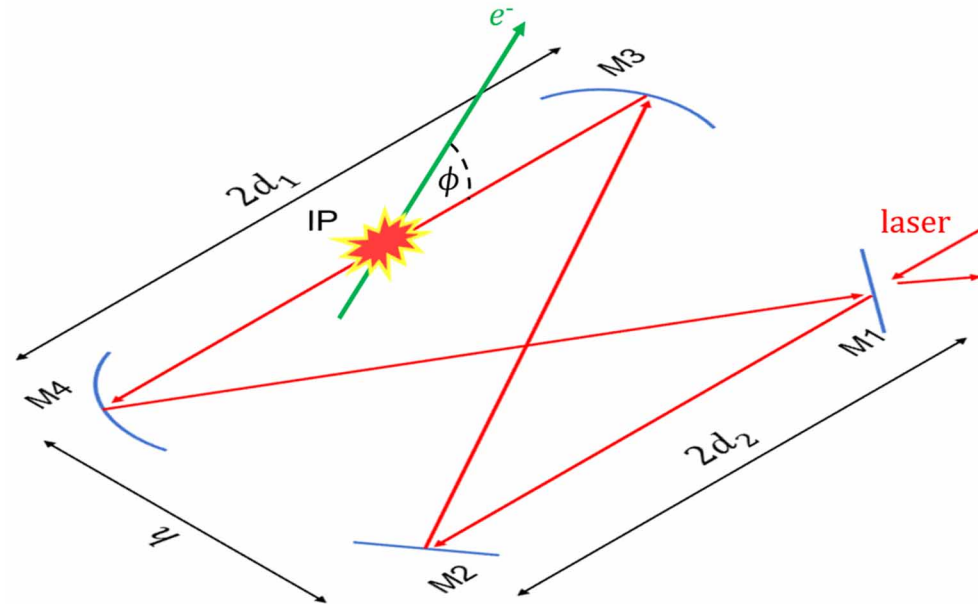
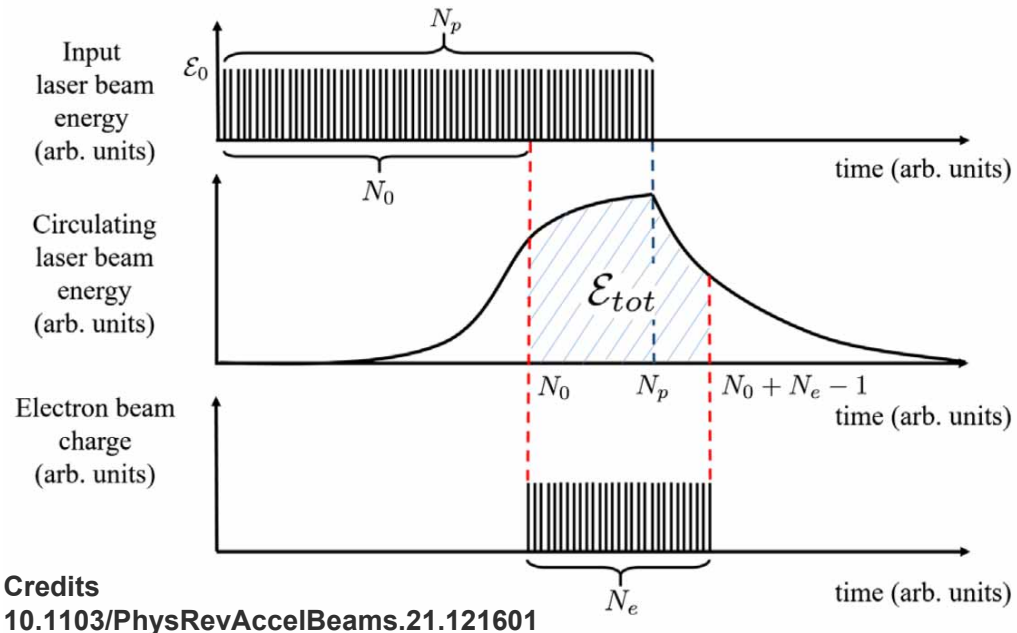
Source size

Annotations:

- ~ Train charge (green circle)
- ~ Laser effective energy (yellow circle)
- Crossing angle ($2^\circ - 5^\circ$) (blue circle)

$$\mathcal{F} \approx N_\gamma f_{eff}$$

Why burst mode operation?

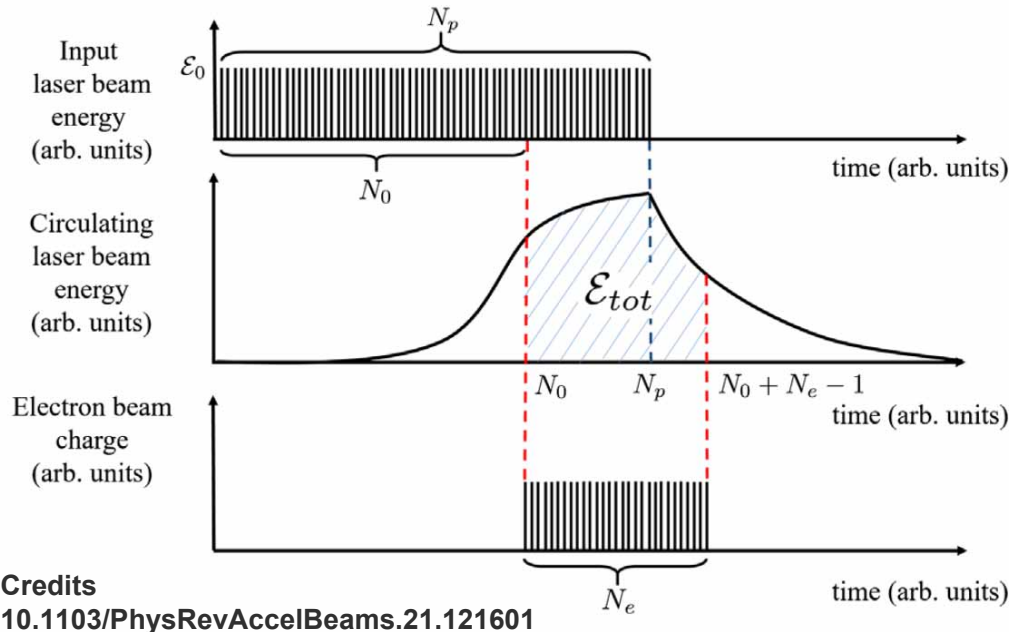


The burst mode operation of a Fabry-Perot cavity:

1. Has a temporal pattern of the laser pulses similar to the incoming electron train.
2. The effective gain is 2 to 3 orders of magnitude larger than for the continuous wave mode.
3. Due to the lower intracavity average power, thermal effects on the cavity mirrors are minimised.

- A planar bowtie cavity was chosen, providing good stability of the resonator modes.
- The electron train interacts with the intracavity laser beam with a crossing angle ϕ .

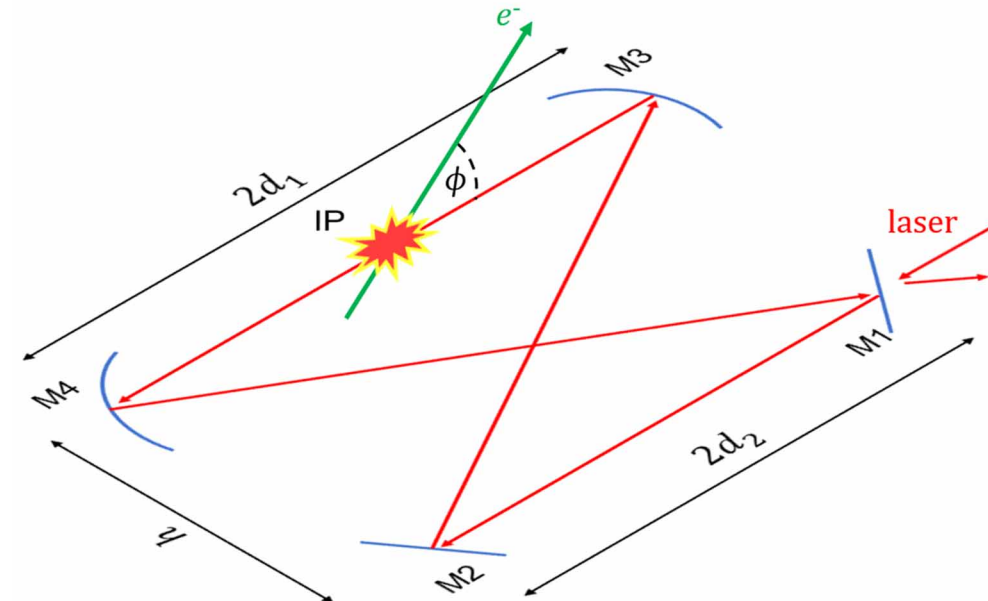
Why burst mode operation?



Maximisation of the number of laser photons for the interaction



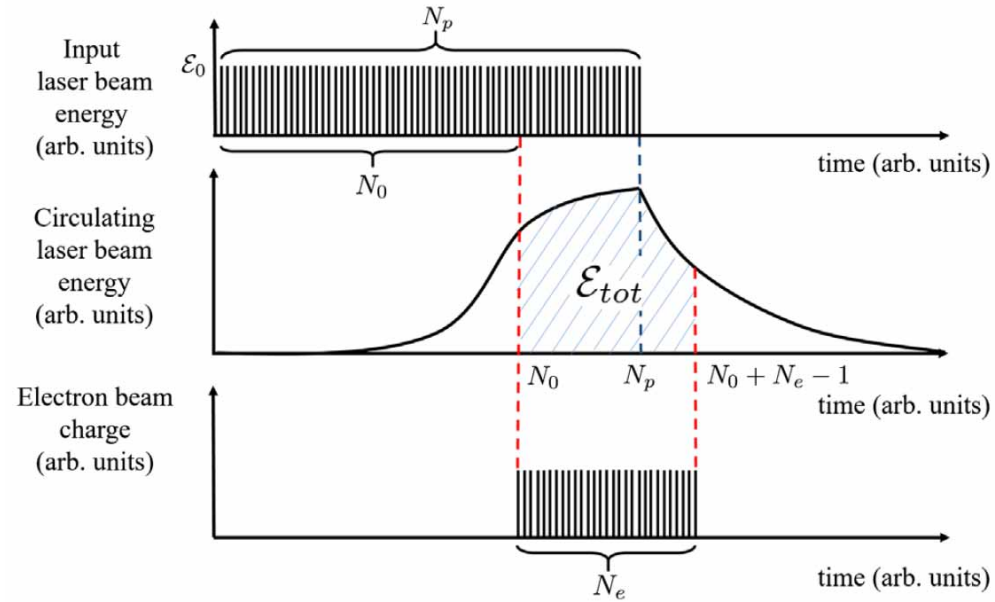
Optimisation of the burst mode parameters



Minimisation of the laser waist size at the IP & maximisation of the macropulse energy



Optimisation of the geometrical parameters



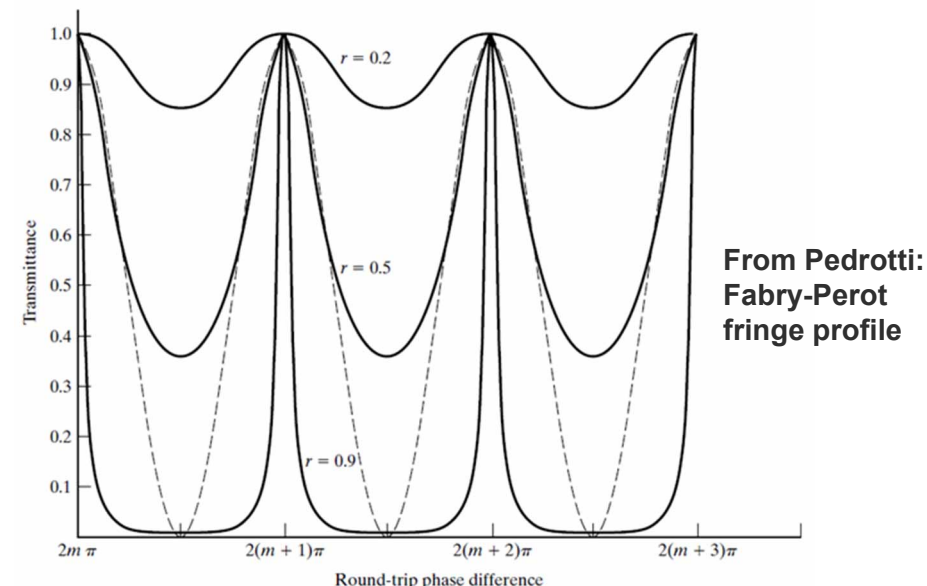
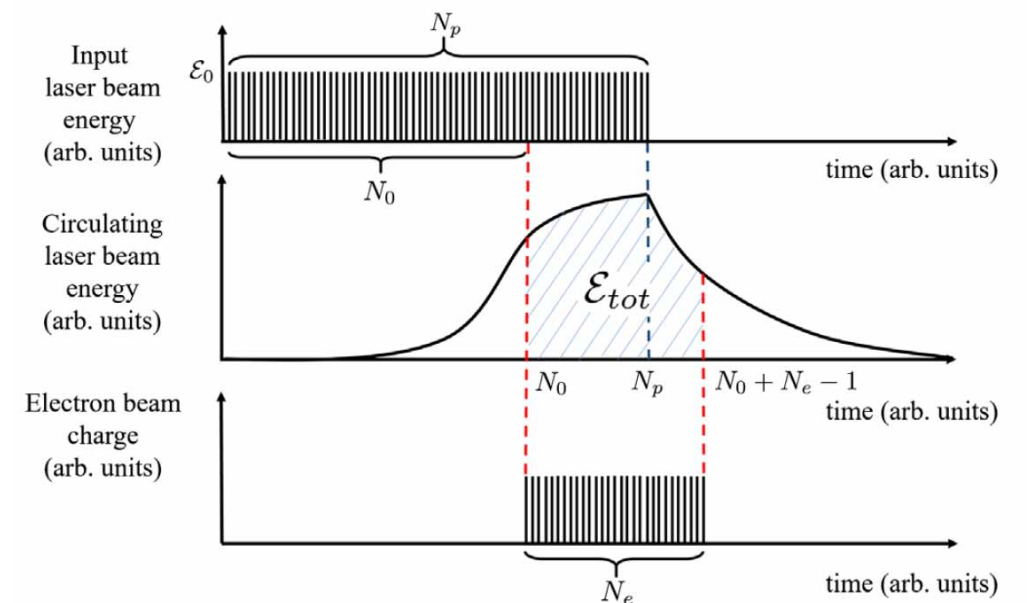
Burst mode optimisation

Burst mode FPC optimisation

The laser circulating power determines the effective energy

$$\mathcal{E}_{tot} = \epsilon(N_p, N_0, N_e, F)N_p\mathcal{E}_0$$

- Flux increases linearly with \mathcal{E}_{tot} .
- $N_p\mathcal{E}_0 = U$ is limited by the FPC geometry (mirror LIDT).
- Input: the number of electron bunches per train
- A large finesse (F) allows for more laser pulses to be stored in the cavity → larger \mathcal{E}_{tot} .
- High finesse cavities (e.g., $F > 10000$), require precise laser matching and mirror tuning → restrict the maximum finesse to 1000.



Optimisation strategy: burst mode parameters

Previous study

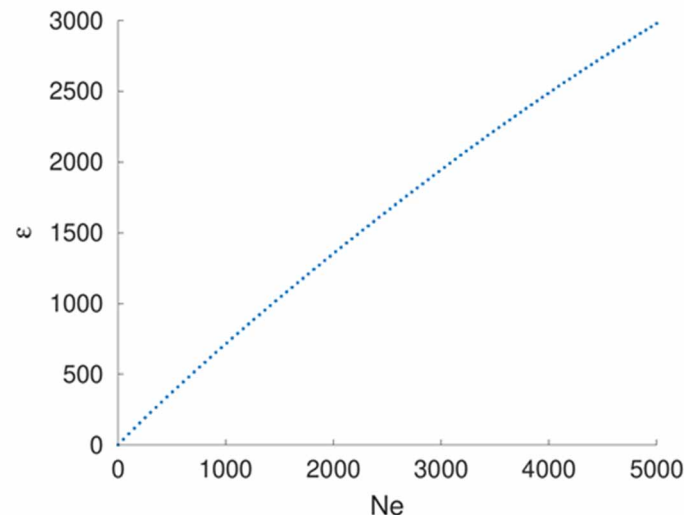
$$\mathcal{E}_{tot} = \epsilon(N_p, N_0, N_e, F) N_p \mathcal{E}_0$$



Nb electron bunches



$$\epsilon = \frac{T_1}{(1-r)^2} \left(1 - \frac{N_0}{N_p} + \frac{2r(r_p^N - r_0^N)}{N_p(1-r^2)} + \frac{(1-r_0^N)^2 - r^{2N_e} r^{2N_0} (1-r^{-N_p})^2}{N_p(1-r^2)} \right)$$



Laser input parameters

Previous study: Aurélien Martens,
10.1103/PhysRevAccelBeams.21.121601



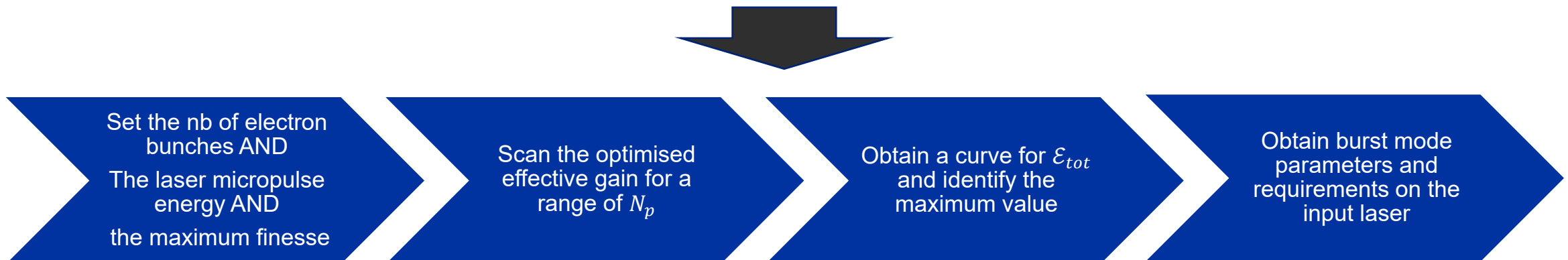
Optimisation strategy: burst mode parameters

Current study

$$\mathcal{E}_{tot} = \epsilon(N_p, N_0, N_e, F) N_p \mathcal{E}_0$$

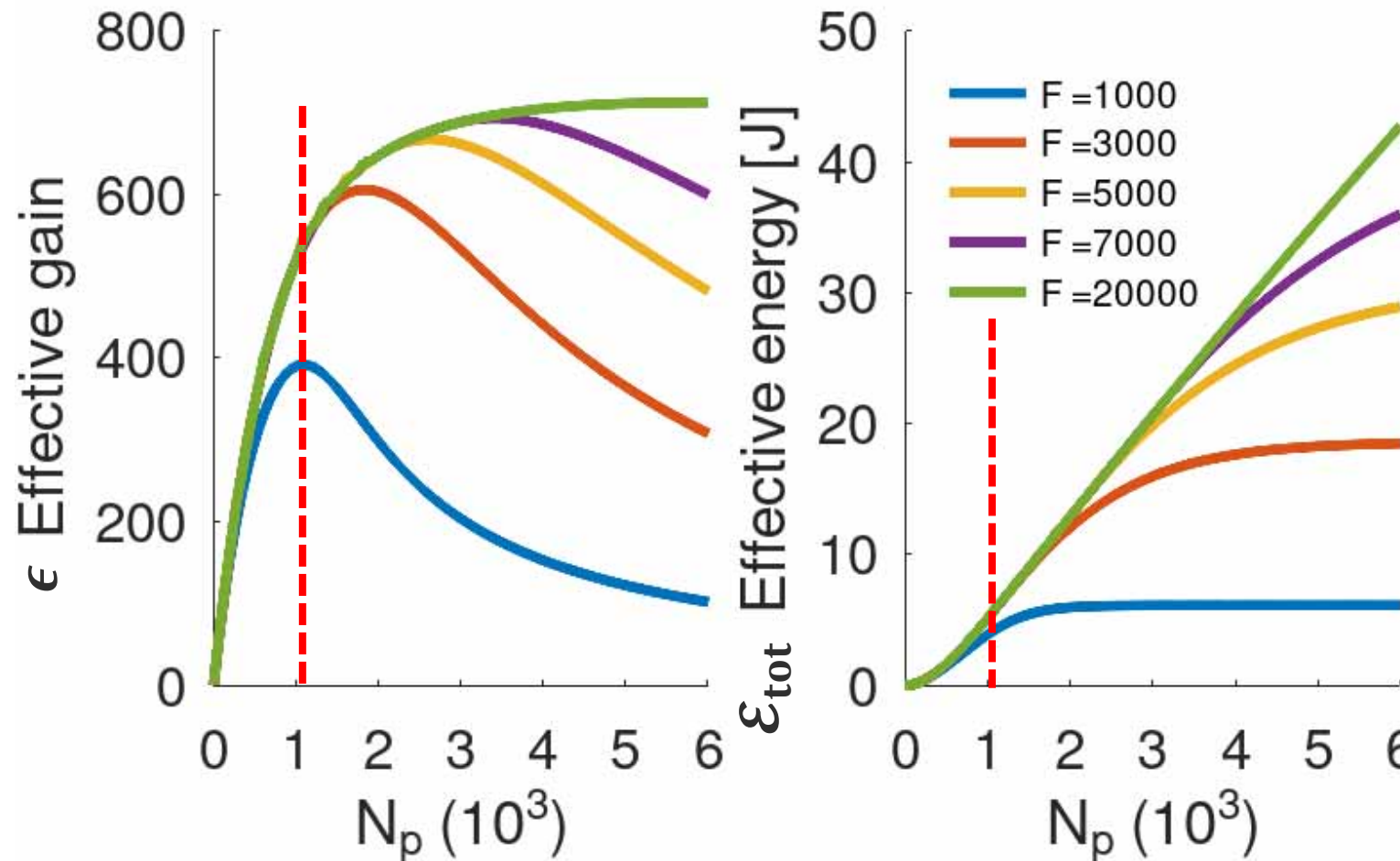
The previous study presents some issues:

1. The ϵ was maximised by tuning N_p , N_0 , and F , although there is a missing N_p term.
2. The \mathcal{E}_0 is treated as a free variable, although it is fixed by the input laser.
3. The maximisation of ϵ does not correspond to a global maximum of \mathcal{E}_{tot} .



Parametric scans of the effective energy and the effective gain

$$\mathcal{E}_{tot} = \epsilon(N_p, N_0, N_e, F) N_p \mathcal{E}_0$$

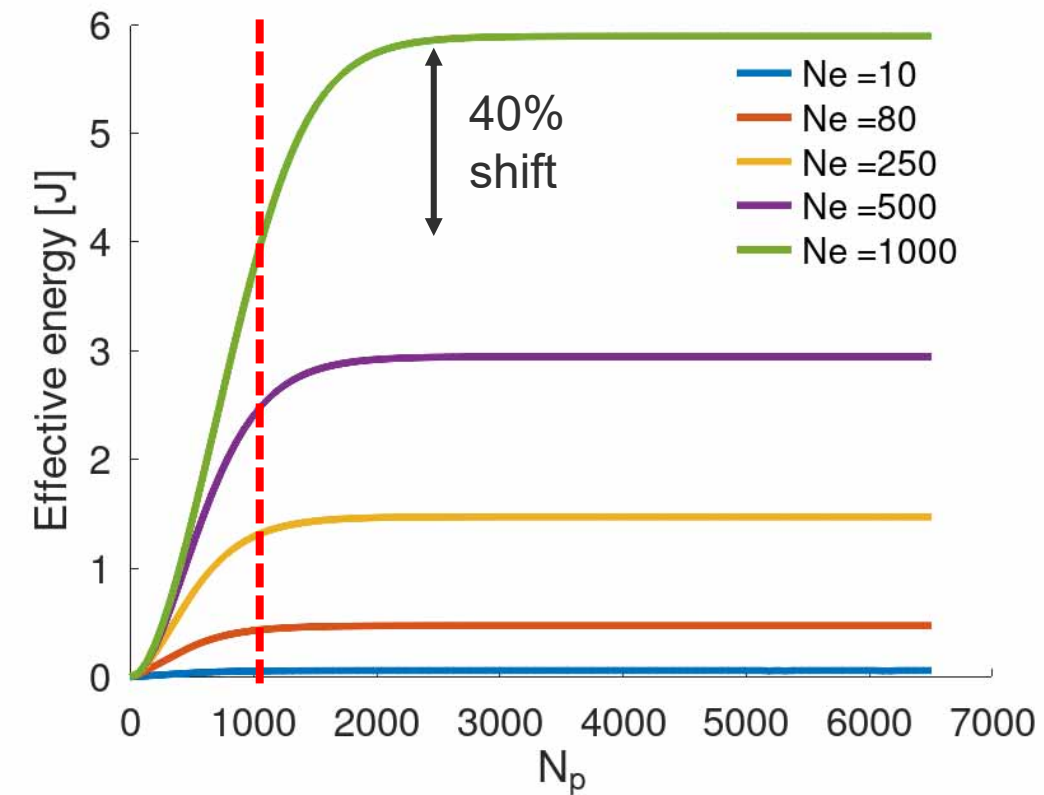
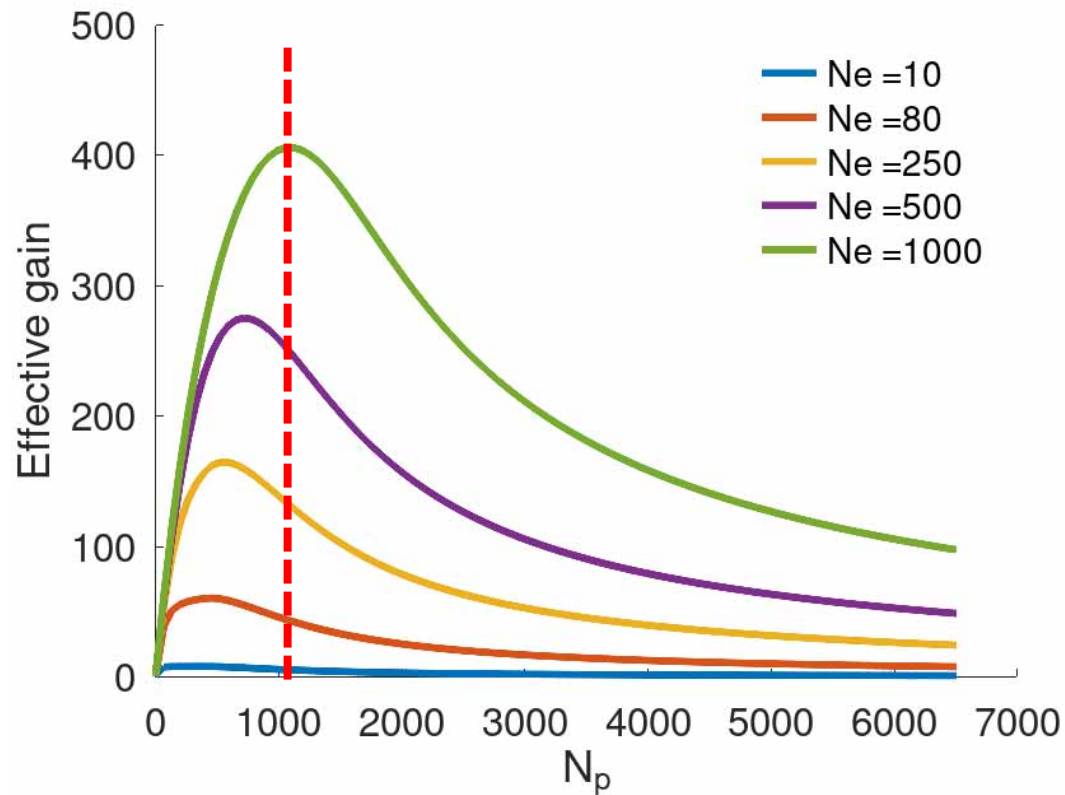


- For any F , ϵ has a local maximum.
- However, \mathcal{E}_{tot} continues to increases past the **point of maximum ϵ** .
- The optimisation of the burst mode parameters should maximise \mathcal{E}_{tot} directly.

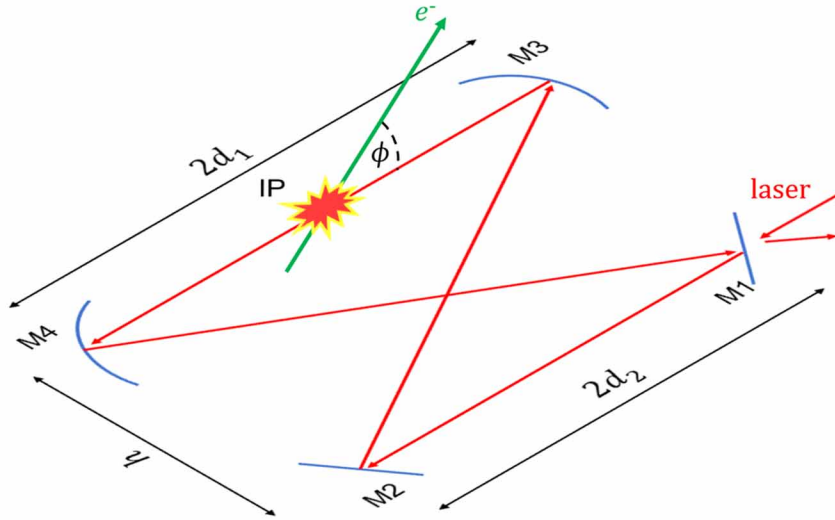
Input: $\mathcal{E}_0 = 10 \mu\text{J}$; $N_e = 1000$

Parametric scans of the effective energy and the effective gain

By choosing the max \mathcal{E}_{tot} instead of the max ϵ ,
a **40% increase** in the effective energy is obtained.



Input: $\mathcal{E}_0 = 10 \mu\text{J}$; $F_{\max} = 1000$



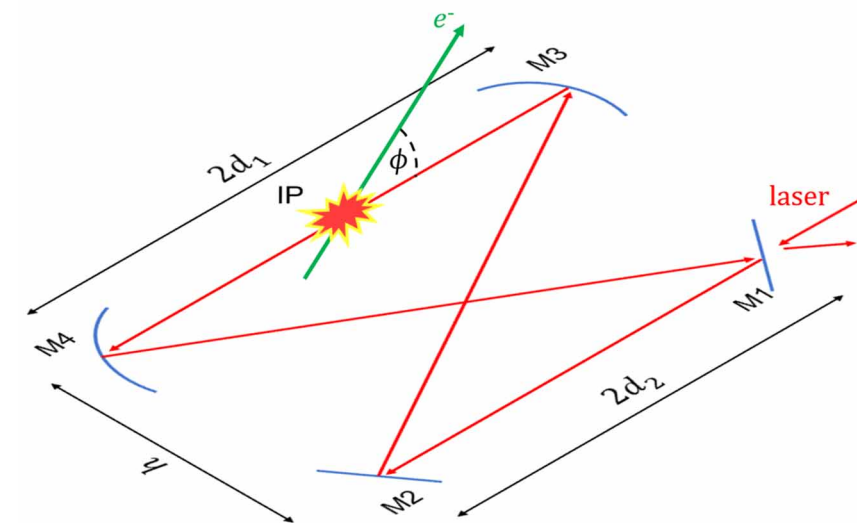
Geometry optimisation

Inputs and requirements

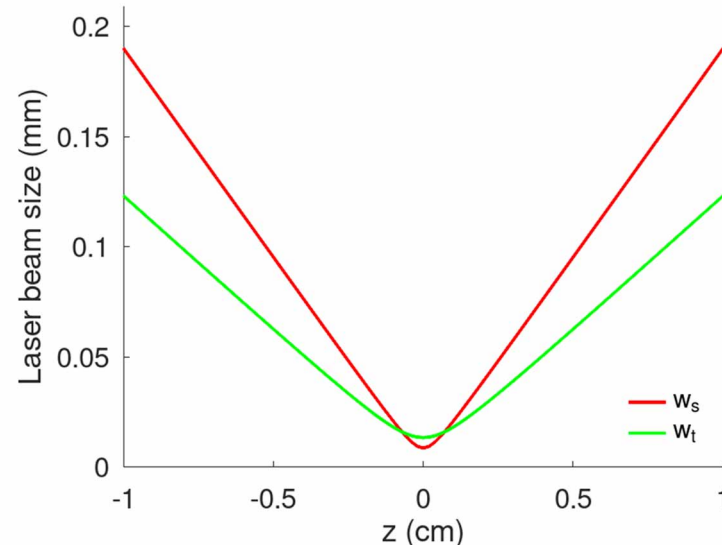
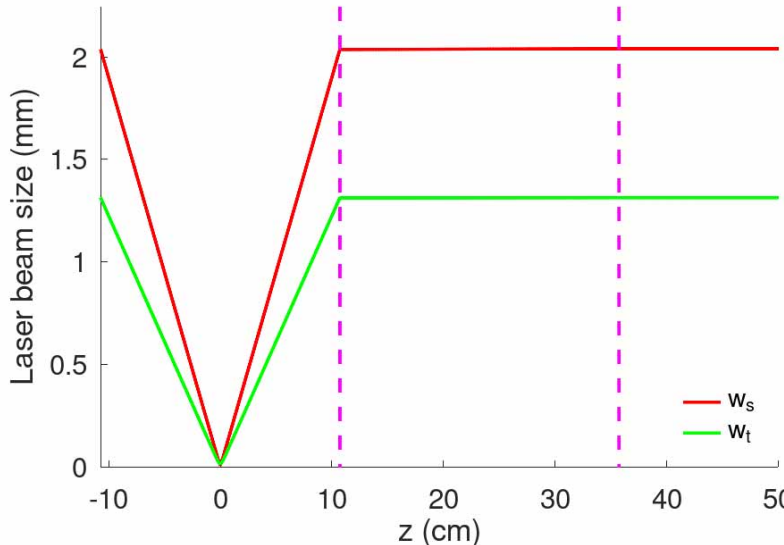
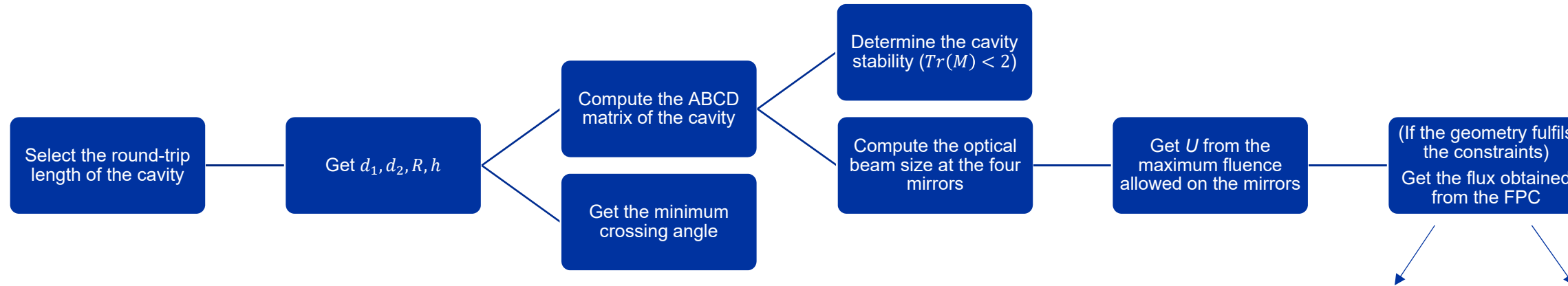
- To maximise flux, Fabry-Perot cavities require a small waist size at the IP, and a large macropulse energy.
- The only input is the cavity round-trip length (set to a harmonic of the laser pulse repetition rate / electron bunch spacing).
- The previous study used a Monte-Carlo technique for the optimisation; we used the simplex algorithm → four orders of magnitude faster convergence.

Parameter	Symbol	Unit
Roundtrip length	L_{RT}	cm
Cavity height	h	cm
Distance between spherical mirrors	$2d_1$	cm
Distance between planar mirrors	$2d_2$	cm
Radius of curvature	R	cm
Mirror diameter	Φ	deg
Crossing angle	ϕ	deg

Free parameter	Symbol	Constrain
Spherical mirrors spacing	d_1	
Planar mirrors spacing	d_2	$[0, L_{RT}/4]$
Cavity height	h	
Radius of curvature	R	
Mirror diameter	Φ	$h - \Phi > h d_1 - d_2 /(d_1 + d_2)$ $d_1 \tan \alpha > \Phi/2$
Roundtrip length	L_{RT}	$n \times c/(f_{rep}), n \in \mathbb{Z}$
Laser pulse energy	U	$U < \mathcal{F}_{\max} \pi w_s w_t / 2$
Cavity stability		$Tr(M_t) < 2$ $Tr(M_s) < 2$

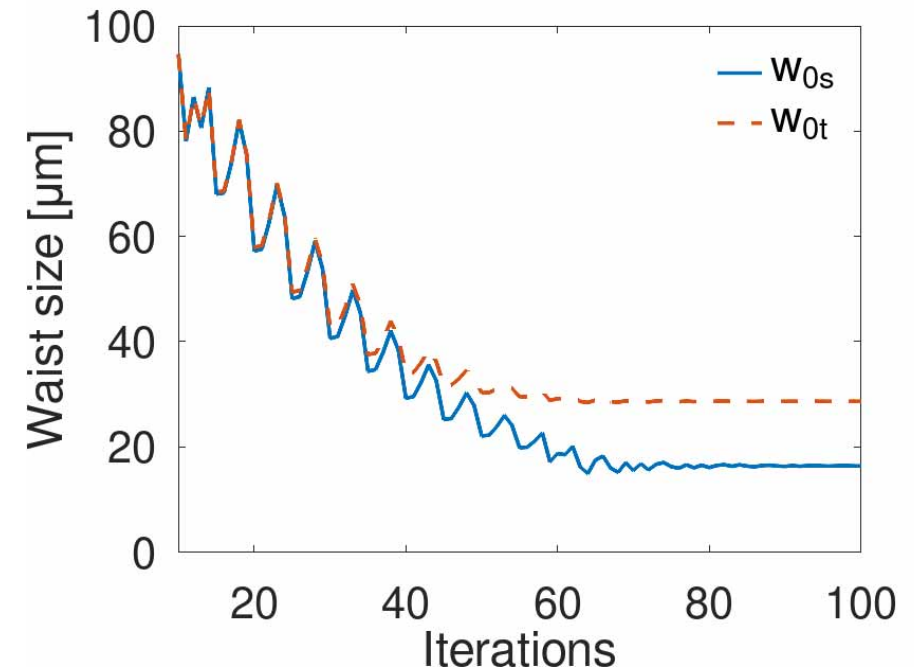
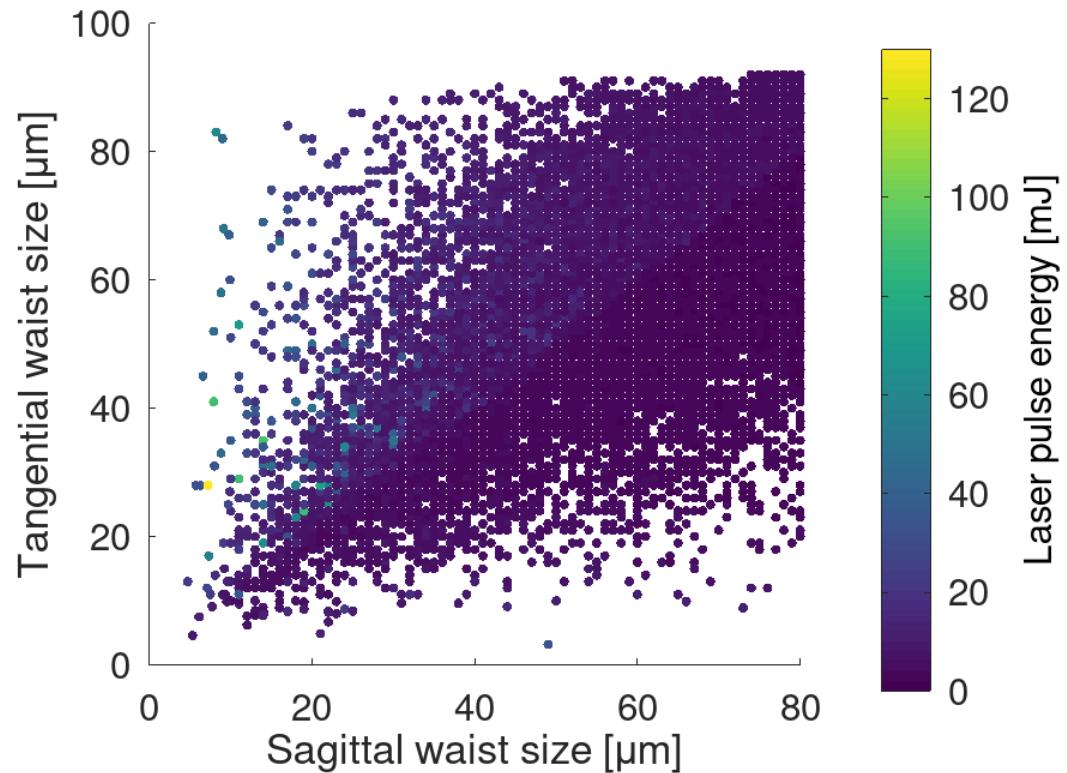


Optimisation strategy: geometrical parameters



Monte-Carlo (previous study)	Simplex (this study)
Generate millions of randomised geometries	Set a merit function maximising flux under the set constraints
Select configuration with the highest flux	Run the optimisation until it converges

Runtime test of Monte-Carlo vs Simplex



Monte-Carlo (previous study)

> 10 million iterations for convergence

Simplex (this study)

< 100 iterations for convergence

The simplex optimisation is more than four orders of magnitude faster than the Monte-Carlo technique

Impact of thermal effects



Thermal lensing

- The performance of the Fabry-Perot cavity can be affected by thermal effects, such as thermal lensing.
- Main contribution to thermal lensing is from the temperature dependence of the refractive index of the optical substrate

$$f_{\text{thermal}} = \frac{2\pi\kappa}{1.3b(dn/dT)l} \frac{w^2}{P} = \frac{1}{m_0} \frac{w^2}{P}$$

Note: m_0 is a material-dependent parameter.

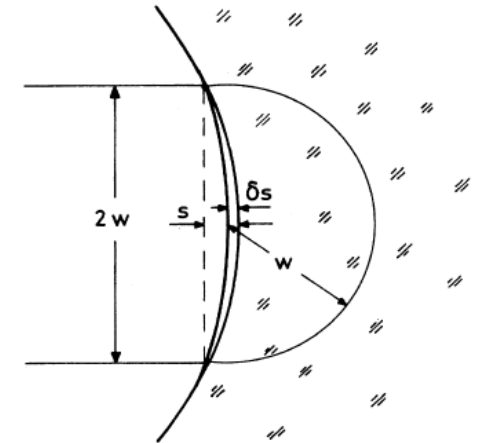
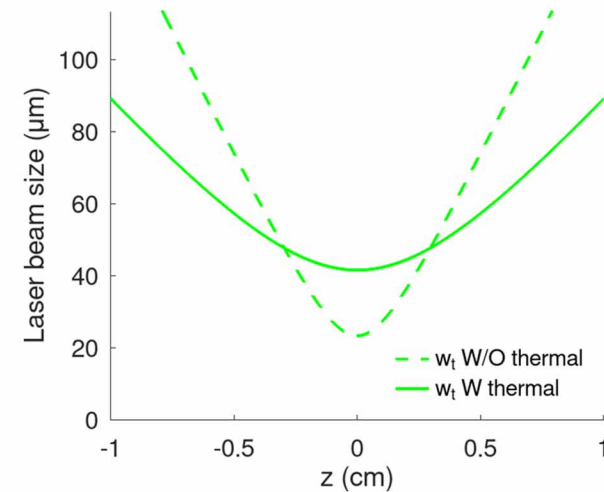
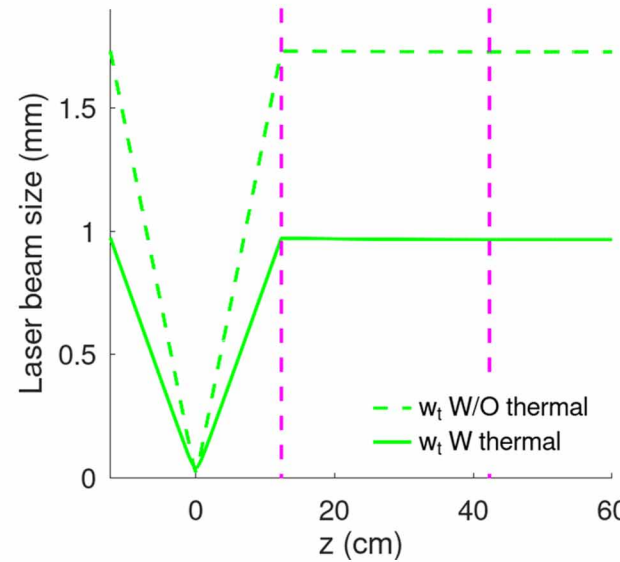
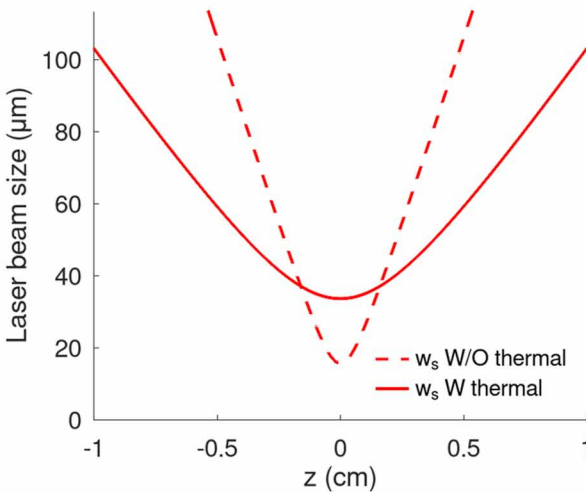
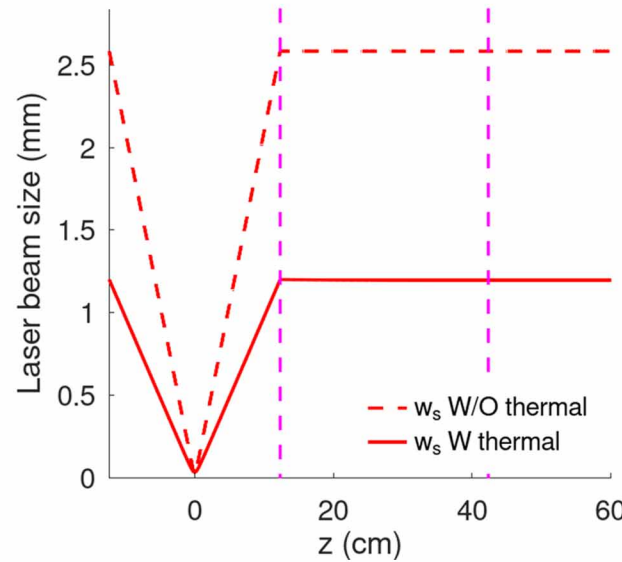


FIG. 1. Absorption of light at the coated surface of optical components is responsible for a temperature gradient across a hemisphere around the reflection spot with radius w . The related thermal expansion of the substrate changes the sagitta s by δs .

From 10.1103/PhysRevA.44.7022

Parameter	Symbol	Unit
Beam power	P	W
Beam waist	w	m
Thermal conductivity	κ	W/(m K)
Temperature dependence of the refractive index	dn/dT	1/K
Thickness of the medium	l	m
Absorption coefficient	b	1/m

Implementation of thermal effects



- Thermal effects were implemented for a cavity with FS substrates.
- The thermal focal length is typically in the 100 - 1000 m range.
- Flux decrease up to 83% from adding thermal effects to a pre-optimised cavity
- Effect can be cancelled by running the optimisation with the thermal effects.

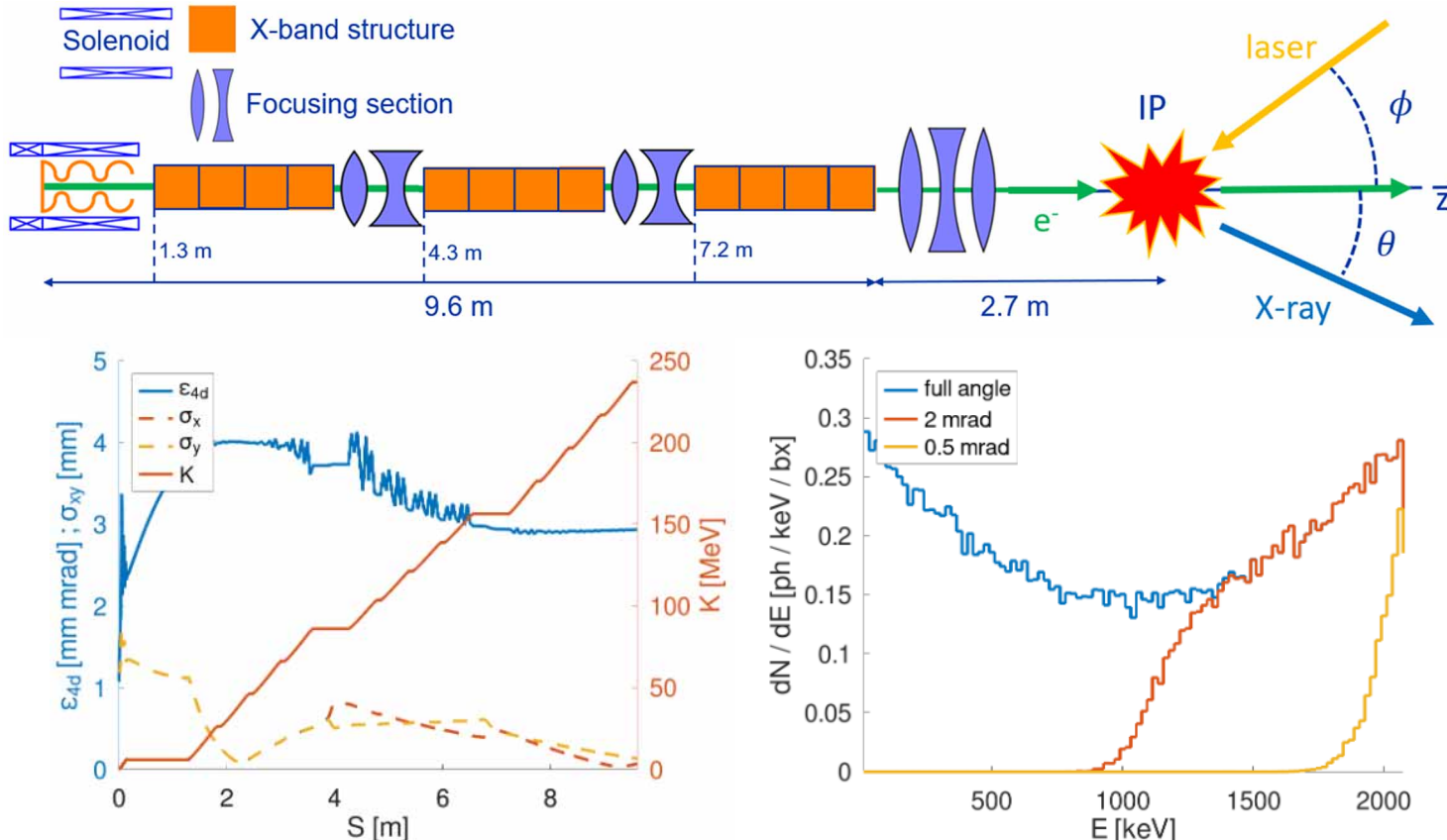
Parameter	Symbol	W/O thermal lensing	W thermal lensing
Waist size sagittal	w_{0s} [μm]	15.6	33.6
Waist size tangential	w_{0t} [μm]	23.3	41.5
Pulse energy	U [mJ]	140	36

83% loss in flux

Example case: HPCI



Baseline Parameters of a High-Pulse Current Injector (HPCI) ICS source (optimised Fabry-Perot cavity)



See talk on Thursday 2 pm by A. Latina, TH4A2

Parameter	Value	Unit
Round-trip length	1	m
$2d_1, 2d_2, h, R$	21.43, 28.54, 1.16, 21.46	cm
N_p, N_0, F	2292, 1298, 1000	
w_{0s}/w_{0t}	8.6/13.4	μm
Effective gain	264	
Effective energy	6	J
Colliding Laser	Value	Unit
Wavelength	515	nm
Pulse energy	10	μJ
Pulse length	1.2	ps
Crossing angle	2	°
Outcoming Photons	Value	Unit
Compton edge	2.1	MeV
Total flux, \mathcal{F}	2.2×10^{13}	ph/s
Bandwidth (0.5 mrad)	2.0	%
Flux (0.5 mrad)	1.6×10^{12}	ph/s
Average Brilliance, \mathcal{B}	4.4×10^{13}	(1)
Peak Brilliance, $\hat{\mathcal{B}}$	3.9×10^{23}	(1)

(1) ph/(s mm² mrad² 0.1%BW)

Conclusions

Significant improvements were made for the optimisation of a burst-mode operated Fabry-Perot cavity.

The goal of the optimisation is to provide the maximum possible flux, with state-of-the-art technology.

Burst parameters optimisation: By maximising the effective energy of the cavity, an increase in the total flux of more than 40% was obtained.

Geometry optimisation: By using the simplex algorithm, the computation runtime was reduced by more than four orders of magnitude. Thermal effects were implemented in the geometrical optimisation.

Example case: The present considerations can be used to design high-intensity linac-based ICS sources. By applying this optimization to the HPCI source, a total flux of 10^{13} ph/s could be obtained.